Monthly Notices of the ROYAL ASTRONOMICAL SOCIETY

MNRAS **552,** 1–10 (2026)
Advance Access publication 2026 September 30

https://doi.org/10.1093/mnras/stag1839

Heavy black hole seed survivors in dwarf galaxies: a case study of Leo I

Matthew T. Scoggins [1]★ Zoltán Haiman [1,2,3] and Fabio Pacucci [4,5]

[1]*Department of Astronomy, Columbia University, New York, NY 10027, USA*
[2]*Department of Physics, Columbia University, New York, NY 10027, USA*
[3]*Institute of Science and Technology Austria (ISTA), Am Campus 1, Klosterneuburg, Austria*
[4]*Center for Astrophysics | Harvard & Smithsonian, 60 Garden St, Cambridge, MA 02138, USA*
[5]*Black Hole Initiative, Harvard University, 20 Garden St, Cambridge, MA 02138, USA*

Accepted 2026 September 15. Received 2026 August 27; in original form 2025 November 6

ABSTRACT

High-redshift supermassive black holes (SMBHs) have challenged our understanding of black hole formation and growth. The 'heavy-seed' pathway eases the problem with the progenitors of these SMBHs having birth masses up to $\sim 10^5 M_\odot$. Here, we investigate the possibility that a local dwarf galaxy, Leo I, harbours a heavy-seed descendant. Using Monte Carlo merger trees to generate the merger histories of 1000 dark matter haloes similar to the Milky Way (MW), we search for Leo-like satellite haloes and investigate the probability that the progenitors of these satellites formed a heavy seed. We derive the likelihood of such 'heavy-seed survivors' (HSSs) across various formation and survival criteria as well as Leo-similarity criteria. We find that the virial temperature for the onset of atomic cooling and rapid gas infall that yields heavy seeds, $T_{\rm act}$, has the largest impact on HSS frequency. We find HSSs in a fraction 0.7 per cent, 18.1 per cent, and 96.5 per cent of MW-like haloes when $T_{\rm act}$ is set to 9000, 7000, and 5000 K, respectively. For the canonical atomic-cooling threshold ($T_{\rm act} \gtrsim 8000$ K), the HSS fraction is $\lesssim$1 per cent, indicating that Leo I hosting a heavy-seed descendant is unlikely under well-motivated physical assumptions. Higher HSS fractions occur only under optimistic and currently unsubstantiated assumptions on $T_{\rm act}$. Nevertheless, these results motivate future work that clarifies the possibility of heavy-seed BH formation in pristine haloes with nominal virial temperatures below 8000 K. This may motivate Leo I as a target for disentangling heavy seeds from other SMBH formation mechanisms.

Key words: black hole physics – galaxies: dwarf – galaxies: evolution – galaxies: individual: Leo I – early Universe.

1 INTRODUCTION

The origin of supermassive black holes (SMBHs) heavier than $\sim 10^9 M_\odot$ powering quasars at redshift $z \geq 6$ remains poorly understood (X. Fan et al. 2001, 2003; D. J. Mortlock et al. 2011; X.-B. Wu et al. 2015; E. Bañados et al. 2018; X. Yang et al. 2020; F. Wang et al. 2021). There are more than 200 detections of these SMBHs (for recent compilations, see S. E. I. Bosman 2022 and X. Fan, E. Bañados & R. A. Simcoe 2023).

The *James Webb Space Telescope* (*JWST*) has recently unveiled a new class of high-z galaxies, named the Little Red Dots (Y. Harikane et al. 2023; D. D. Kocevski et al. 2023; J. F. W. Baggen et al. 2024; C. A. Guia, F. Pacucci & D. D. Kocevski 2024; V. Kokorev et al. 2024; R. Maiolino et al. 2024; J. Matthee et al. 2024; D. D. Kocevski et al. 2025). They are compact high-redshift galaxies thought to host massive black holes, which appear to be overmassive with respect to the local standard relations, suggesting that early black holes got a head start compared to their host galaxies (F. Pacucci et al. 2023b, but see J. Li et al. 2025 for a counterargument to this claim).

Understanding high-z black hole formation and evolution requires a new understanding of the mechanisms for rapid and sustained black hole formation and growth. The solutions to this problem typically fall into two categories: 'light' and 'heavy' seeds (T. Tanaka & Z. Haiman 2009; M. Volonteri 2010; J. L. Johnson & F. Haardt 2016; K. Inayoshi, E. Visbal & Z. Haiman 2020; M. Volonteri, M. Habouzit & M. Colpi 2021; J. Regan & M. Volonteri 2024).

The collapse of gas in primordial dark matter haloes is the precursor to the formation of astrophysical objects in the early Universe. This collapse leads to fragmentation, which forms the first stars. For smaller 'minihaloes' with virial temperature $T_{\rm vir} < 10^4$ K, this leads to the formation of Population III (Pop III) stars (each with mass of $M \sim 10-100 M_\odot$; T. Abel, G. L. Bryan & M. L. Norman 2000; V. Bromm et al. 2001; T. Abel, G. L. Bryan & M. L. Norman 2002; S. Hirano et al. 2014; O. Z. Katz, D. Redigolo & T. Volansky 2025), which then go on to form 'light' seeds. In some (rare) circumstances, gas inside some minihaloes can avoid collapse and grow to the atomic-cooling limit (ACL) where cooling via atomic hydrogen can induce rapid isothermal collapse at $T \sim 10^4$ K, potentially building a supermassive star (SMS) of mass $M \sim 10^3 - 10^5 M_\odot$ (A. Loeb & F. A. Rasio 1994; S. P. Oh & Z. Haiman 2002; V. Bromm & A. Loeb 2003; G. Lodato & P. Natarajan 2006;

★ E-mail: mts2188@columbia.edu

© The Author(s) 2026.
Published by Oxford University Press on behalf of Royal Astronomical Society. This is an Open Access article distributed under the terms of the Creative Commons Attribution License (https://creativecommons.org/licenses/by/4.0/), which permits unrestricted reuse, distribution, and reproduction in any medium, provided the original work is properly cited.

Downloaded from academic.oup.com/mnras/article/552/3/stag1839/8855713 by Institute of Science and Technology Austria user on 19 October 2026

C. Shang, G. L. Bryan & Z. Haiman 2010; J. A. Regan et al. 2020a). If these SMSs formed, they would promptly leave behind 'heavy' black hole seeds. Heavy seeds could also be produced by hyper-Eddington accretion onto a Pop III star black hole remnant (K. Inayoshi, Z. Haiman & J. P. Ostriker 2016; T. Ryu et al. 2016) and runaway collisions in dense proto-clusters (T. C. N. Boekholt et al. 2018; H. Tagawa, Z. Haiman & B. Kocsis 2020; A. Escala 2021; D. R. G. Schleicher et al. 2022; M. C. Vergara et al. 2023; F. Pacucci, L. Hernquist & M. Fujii 2025).

Recent work has focused on developing observational diagnostics. An abnormally high ratio of the luminosity emitted in the He II λ1640 versus the H α line (J. Tumlinson & J. M. Shull 2000; S. P. Oh, Z. Haiman & M. J. Rees 2001; J. L. Johnson et al. 2009, 2010) can diagnose the presence of massive black holes in high-redshift sources. Further, unique spectral signatures in spectral lines and broadband colours (F. Pacucci & A. Ferrara 2015; F. Pacucci & A. Loeb 2019; K. Inayoshi et al. 2022; K. Nakajima & R. Maiolino 2022) and the overmassive black hole relation, where the black hole mass can be comparable or even larger than the total stellar mass, or $M_\bullet/M_* \geq 1$ (M. Volonteri, G. Lodato & P. Natarajan 2008; M. T. Scoggins & Z. Haiman 2024), can distinguish heavy versus light seeds. This overmassive ratio is several orders of magnitude larger than local black hole to stellar mass relations $M_\bullet/M_* \sim 10^{-3}$ (A. E. Reines & M. Volonteri 2015). The heavy-seed pathway may have little or no star formation prior to the formation of the SMS and subsequent black hole, so this mass ratio could initially, at the birth of the black hole, be as high as 10^3. Previous work has focused on estimating the lifetime of this overmassive phase (M. T. Scoggins, Z. Haiman & J. H. Wise 2022; M. T. Scoggins & Z. Haiman 2024), which is expected to decay as the host halo forms stars and/or merges with haloes that have a ratio approaching the low-z values. However, this relation may continue to exist in the case of haloes that experience very few or no mergers, such as in isolated dwarf galaxies, providing a unique opportunity to search for heavy-seed descendants (S. Wassenhove et al. 2010; J. E. Greene 2012; A. Ricarte & P. Natarajan 2018; M. Mezcua et al. 2023; J. A. Regan, F. Pacucci & M. J. Bustamante-Rosell 2023; M. Tremmel et al. 2024). We note that the overmassive feature at low redshift may sometimes arise from complex environmental interactions, rather than heavy seeds (E. J. Weller et al. 2023).

A local dwarf galaxy, Leo I, has recently come into focus for this reason. It has been suggested that Leo I could host an unusually massive black hole (M. J. Bustamante-Rosell et al. 2021; F. Pacucci & A. Loeb 2022; R. Pascale et al. 2024, 2025), with M. J. Bustamante-Rosell et al. (2021) finding evidence for a black hole at 95 per cent confidence with mass $M_\bullet = (3.3 \pm 2.2) \times 10^6$ M$_\odot$. With the total stellar mass estimated to be $M_* = 5.5 \times 10^6$M$_\odot$ (A. W. McConnachie 2012), this black hole appears to be overmassive, with comparable black hole and stellar masses. This is similar to what is expected for heavy-seed black holes near the time of their formation, and motivates a question: *could Leo I be the descendant of a heavy-seed formation site?* In this paper, we address this question, but we caution that the observational evidence remains contested. R. Pascale et al. (2024, 2025) find that no SMBH can be robustly detected with current data quality, and set only a resolution-limited upper limit on the black hole mass. These works highlight that different dynamical modelling approaches applied to the same data set can yield conflicting conclusions, and that the presence of a massive black hole in Leo I cannot yet be considered established. Given this uncertainty, the present work should be understood as exploring the *theoretical plausibility* of Leo I or a similar dwarf galaxy hosting a heavy-seed descendant.

Recently, extremely overmassive black holes have also been found at cosmic noon, extending the track of such objects from the epochs probed by *JWST* (i.e. $4 \lesssim z \lesssim 10$) towards the local Universe. For example, M. Mezcua et al. (2024) found 12 SMBHs that are hosted by low-mass galaxies with masses 1–2 orders of magnitude above the local scaling relations.

Whether Leo I is truly overmassive or even hosts a black hole is still not settled. Although dwarf galaxies can be susceptible to tidal stripping depending on their orbital history (G. Battaglia, A. Sollima & C. Nipoti 2015; G. Iorio et al. 2019; P. Di Cintio et al. 2024), Leo I appears to have had few mergers in its history. It went through a period of intense star formation but has since run out of gas, and star formation has been mostly quenched (C. Gallart et al. 1999; F. Pacucci, Y. Ni & A. Loeb 2023a). This means that Leo I has had very little change in black hole and stellar mass over Gyr time-scales, making it a promising 'fossil' to study the overmassive relation established in the early Universe.

To determine the likelihood of Leo I hosting a heavy-seed remnant, we use Monte Carlo dark matter merger trees and a semi-analytic model previously developed in M. T. Scoggins & Z. Haiman (2024). We estimate the chance that a heavy seed could survive mergers and end up in a halo similar to Leo I, which we dub 'heavy-seed survivor' (HSS). This model estimates the frequency of HSSs in a dwarf galaxy similar to Leo I by searching haloes near $z \sim 30$ that avoid early fragmentation and reach the atomic-cooling limit without prior star formation, where runaway collapse forms an SMS and a prompt heavy-seed remnant black hole. Applying this model to 1000 merger trees and tracking haloes near redshift $z = 0$ that share the properties similar to Leo I allows us to estimate the fraction of Leo-like satellite haloes that could have evolved from a heavy-seed hosting galaxy (HSS).

The rest of this paper is organized as follows. In Section 2 we describe our methods. In Section 3 we present our results. In Section 4 we discuss these findings. Finally, we summarize our conclusions and the implications of this work in Section 5.

2 METHODS

In this section, we summarize the generation of our Monte Carlo dark matter halo merger trees, our heavy-seed selection criteria within these merger trees, our selection for Leo-like candidates within these heavy-seed hosting branches, and our prescription for stellar mass and black hole growth. This work assumes the following cosmological parameters: $\Omega_\Lambda = 0.693$, $\Omega_m = 0.307$, $\Omega_b = 0.0486$, $\sigma_8 = 0.81$, and $h = 0.67$ (Planck Collaboration 2020).

2.1 Monte Carlo merger trees for dark matter haloes

We generate 1000 Monte Carlo merger trees for dark matter haloes based on the Extended Press–Schechter theory (W. H. Press & P. Schechter 1974), following the algorithm in H. Parkinson, S. Cole & J. Helly (2007), which is a modified version of the algorithm used in the GALFORM semi-analytic galaxy formation model (S. Cole et al. 2000). This code generates merger trees by recursively splitting haloes into progenitors according to the conditional mass function of the Extended Press–Schechter formalism, with the H. Parkinson et al. (2007) modification introducing corrections to better reproduce the progenitor mass functions measured in N-body simulations. The trees track the full branching history of each halo from $z = 0$ back to high redshift,

Downloaded from academic.oup.com/mnras/article/552/3/stag1839/8855713 by Institute of Science and Technology Austria user on 19 October 2026

until the halo mass drops below the user-set resolution limit, recording halo mass and redshift at each node. In order to find Leo-like candidates, we look for satellite haloes near redshift z=0 in the branches of a parent halo at redshift z=0 with a mass and age similar to the Milky Way (MW). This sets the parent mass of our merger tree to 9×10^{11}M$_\odot$, at redshift z=0. We set a redshift step size of dz=0.166, with a minimum mass and mass resolution of 10^5M$_\odot$, where star formation is unlikely in (mini)haloes less massive than this (M. Kulkarni, E. Visbal & G. L. Bryan 2021; A. T. P. Schauer et al. 2021).

2.2 Identifying heavy-seed sites and Leo candidacy

Here, we briefly summarize the model of M. T. Scoggins & Z. Haiman (2024) that was used in this work. To achieve the intermediary SMS and subsequent heavy seed, H_2 cooling must be either suppressed or offset to prevent fragmentation and star formation before reaching the atomic-cooling limit. This can be achieved through combinations of intense Lyman–Werner radiation (with specific intensity $J_{\rm LW}$) which dissociates H_2 (Z. Haiman, M. J. Rees & A. Loeb 1997; M. Dijkstra et al. 2008; M. Dijkstra, A. Ferrara & A. Mesinger 2014; J. Wolcott-Green, Z. Haiman & G. L. Bryan 2017), and dynamical heating via halo mergers (at a rate $\Gamma_{\rm dyn}$) and large baryonic streaming motions ($v_{\rm stream}$) which can prevent gas infall and contraction. If these processes can prevent fragmentation until the atomic-cooling halo stage with $T_{\rm vir}\sim10^4$K, the emission of atomic hydrogen will rapidly cool the gas in the halo, leading to isothermal collapse, possibly producing a massive BH seed via an SMS.

In order to estimate the influence of these effects, for every snapshot in the merger tree, we calculate the cooling time $t_{\rm cool}$ and compare it to the Hubble time $t_{\rm Hubble}$. Our model for the cooling time is dependent on Lyman–Werner radiation and dynamical heating. Here, we briefly summarize the calculation of our haloes' Lyman–Werner radiation background and dynamical heating effects, and refer the reader to sections 2.2 and 2.3 in M. T. Scoggins & Z. Haiman (2024) for full details. Following equation (5) of M. T. Scoggins & Z. Haiman (2024), we calculate the mean Lyman–Werner intensity expected to be experienced by every halo in our merger trees, $\bar{J}_{\rm LW}(M_{\rm halo}, z)$. This captures the mean, but it is expected that the haloes that form heavy seeds will experience $J_{\rm LW}$ at the extreme end of the distribution ($J_{\rm LW}\gtrsim10^3J_{21}$; e.g. C. Shang et al. 2010; S. C. O. Glover 2015; B. Agarwal et al. 2016; J. Wolcott-Green et al. 2017). To account for the different intensity experienced by every halo, we draw from a numerically determined $J_{\rm LW}$ distribution shown in fig. 9 of A. Lupi, Z. Haiman & M. Volonteri (2021), centred on $\bar{J}_{\rm LW}(M_{\rm halo}, z)$. We do this for every halo above the atomic-cooling threshold (ACT). For haloes just above the ACT, we calculate the ratio $\alpha = J_{\rm LW}/\bar{J}_{\rm LW}$, and the progenitors at and below the ACT are estimated to experience $J_{\rm LW} = \alpha\bar{J}_{\rm LW}$. This accounts for the fact that a halo experiencing unusually high (low) LW flux exists in an overcrowded (underdense) region, and presumably the progenitors of this halo experience a similarly higher (lower) $J_{\rm LW}$ flux. We calculate the dynamical heating rate following equation (1) of J. H. Wise et al. (2019),

$$\Gamma_{\rm dyn} = \frac{T_{\rm halo}}{M_{\rm halo}}\frac{k_{\rm B}}{\gamma-1}\frac{dM_{\rm halo}}{dt}, \quad (1)$$

for adiabatic index $\gamma = 5/3$. Using $J_{\rm LW}$, among other details listed in M. T. Scoggins & Z. Haiman (2024), to calculate the cooling rate, and equation (1) to calculate the heating rate, we can derive an estimate for the net effective cooling time in each halo. We note that this model will underestimate the HSS occurrence rate, as it is still possible for SMSs to form in haloes where cooling via H_2 does occur, as long as they experience rapid mass inflows that allow for the formation of an SMS (T. Hosokawa et al. 2013; L. Haemmerlé et al. 2018; J. H. Wise et al. 2019).

With an estimate for the cooling time for every snapshot, we define two parameters that we explore in this work: The minimum dimensionless cooling time, $\tau_{\rm cool}$, so that the gas inside haloes must have $t_{\rm cool}/t_{\rm Hubble} \geq \tau_{\rm cool}$ to be considered pristine, and the virial temperature that defines the onset of atomic cooling, or the atomic-cooling threshold, $T_{\rm act}$. We consider a halo to be a direct-collapse black hole (DCBH) host candidate at the first snapshot where $T_{\rm vir} \geq T_{\rm act}$ if every progenitor across every branch of this atomic-cooling halo satisfies $t_{\rm cool}/t_{\rm Hubble} > \tau_{\rm cool}$. After reaching $T_{\rm act}$, it is assumed that runaway atomic cooling condenses the cloud and forms an SMS. For a given $\tau_{\rm cool}$ and $T_{\rm act}$, we search for haloes that could potentially lead to a heavy seed, and then follow the subsequent evolution of these haloes. We filter these haloes for Leo-like candidacy by analysing the DCBH descendants of these branches. To summarize, our process of searching for HSSs is as follows:

(i) We vary the temperature of the atomic-cooling threshold, exploring a range of $T_{\rm act} \in [0.4, 1]\times10^4$ K.

(ii) We vary the minimum allowed ratio between the cooling time and the Hubble time for all progenitors before the ACT, $\tau_{\rm cool} = t_{\rm cool}/t_{\rm Hubble}$, exploring $\tau_{\rm cool} \in [0.05, 1]$.

(iii) For a given $\tau_{\rm cool}$ and $T_{\rm act}$, we look for DCBH descendants in the merger tree within the virial mass range of Leo I, $(7\pm1)\times10^8$M$_\odot$ (M. Mateo, E. W. Olszewski & M. G. Walker 2008), that exist within the free-fall time of $z = 0$. We note that more recent dynamical analyses find somewhat higher enclosed masses for Leo I (K. Hayashi, M. Chiba & T. Ishiyama 2020; R. Pascale et al. 2024, 2025). Our results should therefore be understood as dependent on this adopted virial mass. As larger haloes are less common, a larger virial mass would result in fewer HSS candidates, and would decrease HSS frequency. This results in a window of $\sim$1 Gyr before $z = 0$, or $t_{\rm ff} = \frac{\pi}{2}\frac{d_{\rm Leo}^{1.5}}{\sqrt{2G(M_{\rm MW}+M_{\rm Leo})}} = 1.090$ Gyr for a Leo–MW separation of $d_{\rm Leo} = 250$ kpc.

(iv) For the DCBH-host haloes with a mass similar to Leo I within a free-fall time of redshift z=0, we filter these haloes according to their merger history. We require that the Leo-like halo has experienced one to three major mergers between $z = 0.1$ and the redshift of the atomic-cooling crossing, as shown by T. Ruiz-Lara et al. (2021), based on the analysis of the star formation history and the age-metallicity relation. This introduces another parameter in our search for HSSs, the minimum mass ratio for a major merger, $q = M_{\rm final}/M_{\rm initial}$, where $M_{\rm final}$ is the mass of the post-merger halo and $M_{\rm initial}$ is the mass of the more massive of the two progenitors immediately before the merger. A value of q close to unity corresponds to an extremely minor merger, while a value of $q = 2$ corresponds to a merger of two nearly identical mass haloes. For completeness, we explore the full allowed range of $1 \leq q \leq 2$.

Although this version of GALFORM does not explicitly track satellite haloes, the Extended Press–Schechter formalism used in this work considers two haloes as 'merged' when they become closely gravitationally bound. T. Tanaka & Z. Haiman (2009) have highlighted that for a host halo that is more than 20 times more massive than its satellite, the infall time is so long that the satellite

Downloaded from academic.oup.com/mnras/article/552/3/stag1839/8855713 by Institute of Science and Technology Austria user on 19 October 2026

Table 1. The values or ranges of several parameters used in this work. These parameters control black hole formation and growth and the HSS criteria.

Parameter	Value/range	Description
$T_{\rm act}$	[4000, 10^4] K	The virial temperature that defines the onset of atomic cooling.
$\tau_{\rm cool}$	[0.05, 1]	The minimum cooling time $t_{\rm cool}/t_{\rm Hubble}$ required for a halo to be considered pristine.
q	[1.0, 2.0]	The minimum mass ratio $M_{\rm final}/M_{\rm initial}$ that defines a major merger.
$f_{\rm cap}$	0.05	The maximum fraction of baryonic material available for black hole formation.
$\tau_{\rm fold}$	45 Myr	Black hole e-folding time.
M_0	$f_{\rm cap}\left(\frac{\Omega_b}{\Omega_m}\right)M_{\rm halo}$	The initial black hole mass. This equation also governs the maximum black hole mass during evolution.

is considered 'stuck' and likely never merges. This justifies our choice of searching for Leo-like haloes within a free-fall time: even though they formally 'merge' in our merger trees at $z = 0$, they are likely to remain long-lived satellites.

We consider a halo to be a Leo-like heavy-seed survivor, or HSS, if it meets all of the above criteria. These parameters are summarized in Table 1.

2.3 Stellar mass and black hole growth

We assign stellar masses to our haloes following J. H. Wise et al. (2014), who derived stellar mass versus halo mass statistics from a cosmological hydrodynamical simulation. In their table 1, they provide $\log(M_{\rm vir})$ and $\log(M_*)$ statistics for $6.5 \leq \log(M_{\rm vir}/{\rm M}_\odot) \leq 8.5$ in 0.5 dex bins. We interpolate across $\log(M_{\rm vir})$ to derive $\log(M_*)$ for a given halo mass and apply this to haloes with $10^{6.5} \leq M_{\rm halo}/{\rm M}_\odot \leq 10^{8.5}$. We note that these statistics are generated from a simulation that ran until $z = 7.3$, but we apply them to haloes with redshift $z \geq 6$. We note that we do not account for the scatter provided by J. H. Wise et al. (2014); however the standard deviations for this fit are less than 0.4 dex.

Black holes are assumed to form shortly after the haloes reach the ACT. The initial seed black hole masses in `Renaissance`, a suite of cosmological radiation-hydrodynamic and N-body simulations (B. W. O'Shea et al. 2015; H. Xu et al. 2016), are estimated to fall within the range $10^4{\rm M}_\odot \leq M_\bullet \leq 10^6{\rm M}_\odot$ where the gravitational collapse to an SMBH is triggered by a relativistic instability. We note that a re-simulation of two of the atomic-cooling haloes in the `Renaissance` suite found lower SMS masses of $M{\approx}10^2 - 10^4{\rm M}_\odot$ (J. A. Regan et al. 2020b), with higher $J_{\rm LW}$ yielding a higher mass. However, the haloes in this re-simulation experienced much smaller $J_{\rm LW}$ fluxes ($\sim 10 J_{21}$) than we investigate in this work ($\sim 10^3 J_{21}$), so we expect our seeds to be more massive. We estimate the initial black hole mass to be some fraction of the baryon mass, $M_0 = f_{\rm cap}\left(\frac{\Omega_b}{\Omega_m}\right)M_{\rm halo}$, with this fractional cap set to $f_{\rm cap} = 0.05$. This typically yields black holes with masses $\sim 10^4{\rm M}_\odot$. The growth of these black holes is assumed to follow the Eddington rate

$$\dot{M}_\bullet = \frac{L_{\rm edd}}{\epsilon c^2} = \frac{4\pi G \mu m_{\rm p} M_\bullet}{\sigma_{\rm T} c \epsilon} = \frac{M_\bullet}{\tau_{\rm fold}}, \quad (2)$$

with speed of light c, gravitational constant G, mean molecular weight μ ($\mu{\sim}0.6$ for fully ionized primordial H + He gas), proton mass $m_{\rm p}$, Thomson cross-section $\sigma_{\rm T}$ and radiative efficiency ϵ. This leads to a black hole mass given by $M_\bullet(t) = M_0 \exp(t/\tau_{\rm fold})$ with e-folding time $\tau_{\rm fold} = (\sigma_{\rm T} c \epsilon)/(4\pi\mu G m_{\rm p}) \approx 450\epsilon$ Myr. Assuming a radiative efficiency $\epsilon \approx 0.1$, we set $\tau_{\rm fold} = 45$ Myr. We additionally quench black hole growth when the mass of the black hole exceeds the prescribed fraction of the baryonic mass in the halo, capping $M_\bullet \leq f_{\rm cap}\,(\Omega_{\rm b}/\Omega_{\rm m})\,M_{\rm halo}$. To summarize, our simple model governs black hole formation and growth through $f_{\rm cap}$, $\tau_{\rm fold}$, $M_{\rm halo}$, and M_0 (which is determined by $f_{\rm cap}$ and $M_{\rm halo}$). These parameters are summarized in Table 1. We start the growth of our black holes immediately after their formation.

3 RESULTS

In Fig. 1, we show $\log_{10}(N_{\rm HSS}/N_{\rm trees})$, the HSS frequency of occurrence for our $N_{\rm trees} = 1000$ dark matter merger trees. We show the results as a function of the three parameters explored here, $\tau_{\rm cool}$, $T_{\rm act}$, and q. We include six plots, each showing the expected number of HSS candidates per tree across two of the three parameters. For a given value along the x and y axes, the left column shows the maximum number of HSSs across the third parameter not shown on the axes. The right column shows the median number of HSSs along this third parameter. We mark the 300 per cent, 100 per cent, 10 per cent, and 1 per cent lines for the expected number of HSSs per tree, shown in black. White space indicates that no HSS candidate was found in our $N_{\rm trees} = 1000$ dark matter merger trees, meaning that the probability of an HSS for that combination of parameters is $<10^{-3}$.

The top row shows the expected number of HSSs across the minimum mass ratio for mergers, q, and the threshold halo virial temperature $T_{\rm act}$ for atomic-cooling, with the left panel showing the maximum value for each pair across $\tau_{\rm cool}$ and the right panel showing the median. We find that, in general, decreasing $T_{\rm act}$ increases the frequency of HSSs. This is because a smaller value of $T_{\rm act}$ focuses on an earlier, lower mass stage in the halo's evolution, reducing the chances for cooling to occur and resulting in fragmentation. However, the frequency is not monotonic across the minimum halo merger mass ratio, and we find that ratios between $q = 1.3$ and 1.6 result in the highest HSS occurrence rates. Although a smaller value of q is less strict, this tends to result in more mergers than our maximum allowed number of mergers, i.e. 3 (recall that we require between 1 and 3 major mergers). For the case of $T_{\rm act}{\sim}0.4{\times}10^4$ K and $q{\sim}1.33$, nearly all of our parent haloes host one or more HSS. As $T_{\rm act}$ approaches $0.7{\times}10^4$ K, the HSS frequency is reduced to ∼10 per cent, or roughly 100 HSSs among our 1000 merger trees. For a larger value, $T_{\rm act}{\sim}0.9{\times}10^4$ K, HSS frequency is less than 1 per cent. The results appear to be similar when comparing the maximum value (left) to the median value (right) across the third parameter, $\tau_{\rm cool}$, signalling that this parameter plays a less significant role in the frequency of HSSs.

The middle row shows the results as a function of $T_{\rm act}$ and $\tau_{\rm cool}$. As expected by the nature of picking the maximum value of $N_{\rm HSS}$ across the third parameter, q, the dependence on $T_{\rm act}$ is similar to the top row, where the probability increases with decreasing $T_{\rm act}$. Although a lower $\tau_{\rm cool}$ for a fixed $T_{\rm act}$ slightly increases the frequency of HSSs, this highlights the weak dependence on $\tau_{\rm cool}$. This is likely due to the large Lyman–Werner radiation experienced by the heavy-seed sites (see fig. 3 of M. T. Scoggins & Z. Haiman 2024). These sites experience abnormally large values of $J_{\rm LW}$, typically being large enough to cause the cooling time to

Downloaded from academic.oup.com/mnras/article/552/3/stag1839/8855713 by Institute of Science and Technology Austria user on 19 October 2026

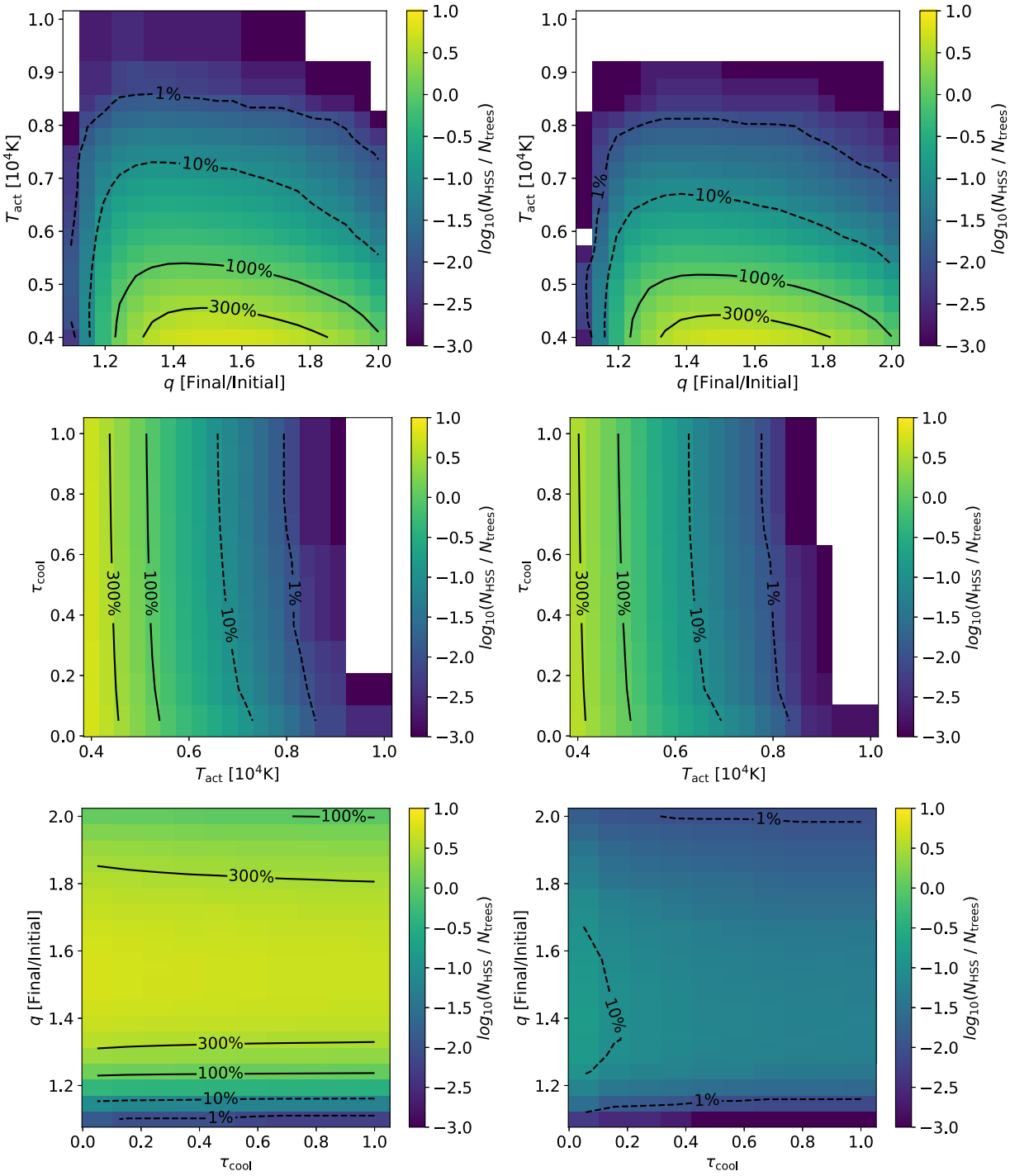


Figure 1. We show $\log_{10}(N_{\rm HSS}/N_{\rm trees})$, the frequency of occurrence of heavy-seed survivors (HSSs), or a Leo-like satellite halo hosting a DCBH descendant, as a function of the criteria that determine HSS candidacy. This criterion includes the minimum halo mass ratio that determines what constitutes a 'major' merger, q, the virial temperature for the onset of atomic cooling, $T_{\rm act}$, and the minimum allowed cooling time ratio to avoid star formation, $\tau_{\rm cool} = t_{\rm cool}/t_{\rm Hubble}$. An HSS is formed if a Leo-like halo hosts a DCBH (requiring the progenitors of a subhalo at $T_{\rm vir}$=$T_{\rm act}$ to avoid any prior star formation), and that after forming the DCBH, the subhalo experiences one to three 'major' mergers with mass ratio above q. Each panel explores two parameters at a time, with the left column showing the value of $\log_{10}(N_{\rm HSS}/N_{\rm trees})$ selected to be the maximum for any value of the third parameter, and the right column showing the median across this third parameter. Lines denote 1 per cent, 10 per cent, 100 per cent, and 300 per cent rates for HSS frequency in our trees. White spaces indicate that no HSS was found among our $N_{\rm trees} = 1000$ merger trees, so the probability of an HSS existing for a given parameter combination is less than 10^{-3}. In some cases, there can be three or more HSSs per tree. The HSS frequency has a soft dependence on $\tau_{\rm cool}$, as our haloes experience large values of $J_{\rm LW}$ with $\tau_{\rm cool}$ typically greater than 1, so increasing $\tau_{\rm cool}$ does not significantly decrease the number of HSSs. There is a non-linear dependence on q, where a large value of q can result in too few major mergers, violating the Leo-like criteria, and a small value of q results in too many mergers. The results have the strongest dependence on $T_{\rm act}$, as decreasing this value increases HSS rates significantly.

Downloaded from academic.oup.com/mnras/article/552/3/stag1839/8855713 by Institute of Science and Technology Austria user on 19 October 2026

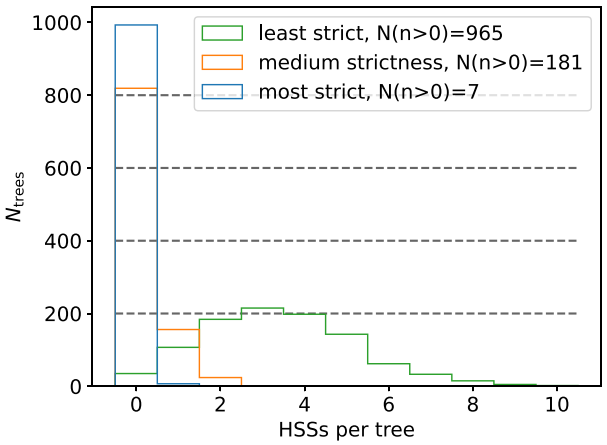


Figure 2. The distribution of the number of HSSs in our 1000 merger trees. The three cases represent varying degrees of strictness in our three parameters, q, T_{act}, and τ_{cool}, with the values of these parameters listed in Table 2. In the least strict case (green), 96.5 per cent of our trees hold at least one HSS, though it is much more common for the trees to have several HSSs. One tree holds as many as 10 HSSs. For the medium case (orange), 18.1 per cent of our trees hold an HSS, with two being the upper limit of HSSs per tree. In the strictest case (blue), only 0.7 per cent of our trees have HSSs. This stricter case is the most physically realistic, though future work will be needed to put tighter constraints on the most appropriate T_{act} for rapid gas collapse in atomic-cooling haloes.

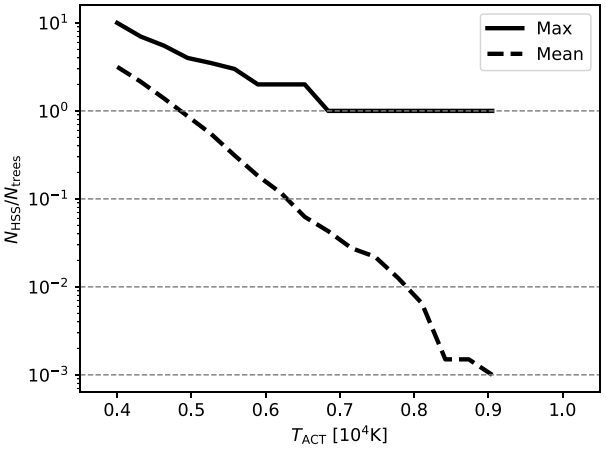


Figure 3. We show the HSS frequency as a function of T_{act}, the most influential parameter for HSS candidacy. For every tree, we take the median value (dashed) across q and τ_{cool} for each target T_{act}, then average these results across the 1000 merger trees. We also show the maximum number of HSSs (solid) across the 1000 trees. For low values of T_{act}, trees typically host three HSSs, up to a maximum of 10. With increasing T_{act}, HSSs become rare, and for $T_{act} \gtrsim 5000$ K, the mean essentially represents the probability of finding a single HSS. We do not find an HSS among any of our 1000 realizations for $T_{act} > 9000$ K. The plateau in the maximum number of HSSs signals that from T_{act}∼7000 K up to T_{act}∼9000 K, there is no more than one HSS in the median value across q and τ_{cool}.

Table 2. The three cases shown in Fig. 2 that define the minimum criteria required for HSS candidacy.

Strictness	q	T_{act} (K)	τ_{cool}
Least	1.4	5000	0.5
Medium	1.4	7000	0.75
Most	1.4	9000	1.0

exceed the Hubble time for the majority of our haloes. This means that a lower value of τ_{cool} yields little increase in HSS frequency.

The bottom row explores the HSS frequency as a function of τ_{cool} and q. On the left, showing the maximum value across T_{act}, the majority of the parameter space finds most haloes that host an HSS, although this maximum value is likely always achieved for a low value of T_{act}. Again, there is little dependence on τ_{cool}, the results across q peak near ∼1.5. A value of q below 1.2 results in so many 'major' mergers that we regularly exceed our maximum allowed number of three, resulting in almost no HSSs. The right panel, which shows the median HSS number across T_{act}, reveals an interesting dependence on τ_{cool} and q, where in this space most of the peak HSS frequency is near q∼1.4 for an extremely small τ_{cool}. For larger values of τ_{cool}, for the optimal q, the HSS frequency drops to ∼5 per cent.

Our results for the total number of Leo-like satellite haloes that host a heavy seed, or heavy-seed survivors (HSS), for three varying levels of strictness are shown in Fig. 2. The criteria that define these three cases are summarized in Table 2. As the number of HSSs depends nonlinearly on q, we have fixed it to the approximately optimal value of $q = 1.4$, allowing our cases to explore the dependence on the other two parameters, τ_{cool} and T_{act}. For the least strict scenario (green), the majority of our trees (965 out of 1000) end up with several HSS candidates, up to 10 HSSs in a single tree. For the medium-strict case, 181 out of 1000 of our trees harbour an HSS. Of these, most have only a single HSS, with a small fraction hosting up to two but no more. Finally, in the strictest case, very few HSSs remain. Only 7 of our 1000 trees have a (single) HSS. Overall, these numbers suggest that under the canonical atomic-cooling threshold ($T_{act} \sim 9000$ K), Leo I hosting a heavy-seed descendant is rare, occurring in only ∼0.7 per cent of merger trees. Higher fractions require progressively more optimistic and less physically motivated assumptions on T_{act}. Even in the strictest case we imposed, Leo I could still host a heavy seed, though such an outcome should be regarded as unlikely rather than typical.

In Fig. 3 we compare the number of HSSs against T_{act}, the most influential parameter for determining how many HSSs end up in an MW-like halo. For each merger tree and target T_{act}, we select the median number of HSSs across q and τ_{cool}. Then, with the median value for each tree, we show the mean (dashed) and maximum (solid) across the 1000 merger trees. This can be thought of as a summary of the information in the top four panels of Fig. 1. For low values of T_{act}, we find that there are typically three or more HSSs per tree, but as we approach a more realistic value T_{act}∼7000 K, there are roughly 50 HSSs across the 1000 trees. Above 9000 K, there are no HSSs. The solid black line shows that there are a maximum of 10 HSSs in one tree across q and τ_{cool}, though it plateaus to one HSS near T_{act}=7000 K and zero above T_{act}∼9000 K.

In Fig. 4, we show the evolution of our HSS candidate black holes for branches that resulted in HSS candidacy for the least strict case. Although such a low T_{act} for atomic cooling and DCBH formation is unlikely to be realistic, as the onset of atomic cooling typically requires $T_{act} \gtrsim 8000$ K, the halo evolution is similar in the stricter scenarios, and this allows us to see a larger sample size of black holes. In the left panel, we show black hole mass

Downloaded from academic.oup.com/mnras/article/552/3/stag1839/8855713 by Institute of Science and Technology Austria user on 19 October 2026

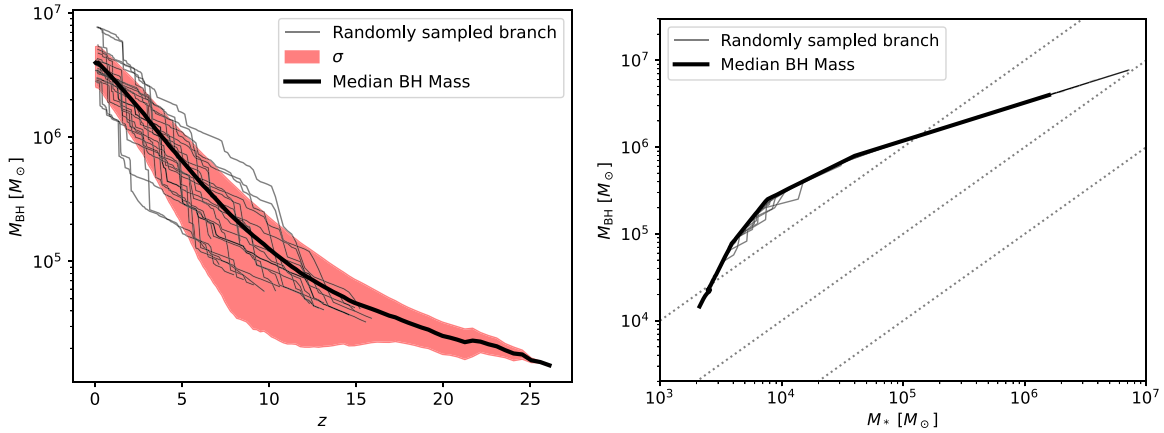


Figure 4. *Left:* The evolution of the masses of black holes born as heavy seeds in our models. We show the median black hole mass (black), a few randomly sampled branches of the merger tree of an MW-like halo (grey) and the black hole mass standard deviation versus redshift (red). The median black hole mass near redshift z=0 is $M_\bullet \sim 4\times10^6 M_\odot$, comparable to the estimate by M. J. Bustamante-Rosell et al. (2021). The earliest heavy-seed survivors (HSSs) at high redshift have an initial mass of $M_\bullet \sim 10^4 M_\odot$. *Right:* The black hole versus stellar mass for our HSSs. The HSSs are initially overmassive, with $M_\bullet/M_* \sim 10$, and terminate with $M_\bullet/M_* \sim 1$.

versus redshift, with the median black hole mass shown in black, the standard deviation shown in red, and randomly sampled branches shown in grey. The earliest black hole formation time is near redshift $z = 25$, with an initial heavy-seed mass of $\sim 10^4 M_\odot$. The black holes grow to have a median mass of $\sim 4\times10^6 M_\odot$ near redshift z=0, which closely matches the mass of Leo I's black hole derived by M. J. Bustamante-Rosell et al. (2021). In the right panel, we show the evolution of our black hole mass against the stellar mass of their host haloes. As our black holes grow, they are limited to a fraction of the gas reservoir available in their halo, or 5 per cent of the total baryonic matter. These grow quickly enough that most will soon reach this cap, meaning that black hole mass and stellar mass (which we estimate according to the halo mass) are tightly correlated in this model. Near redshift $z = 0$, most of these satellites have a final BH-to-stellar mass ratio of $M_\bullet/M_* \sim 1$, similar to the ratio observed in Leo I (F. Pacucci et al. 2023a).

4 DISCUSSION

This investigation suggests that the presence of a heavy-seed descendant in Leo I, and in other dwarf satellite galaxies similar to Leo I, is plausible under moderately relaxed DCBH formation conditions. Although the most restrictive cases only yield $\sim$1 per cent of the MW merger trees as HSS hosts, the fraction grows rapidly as the conditions are relaxed, resulting in 18 per cent and 96 per cent HSS frequency for medium and extremely relaxed conditions. This suggests that the main uncertainty in HSS frequency lies in the physics of early halo cooling and fragmentation.

The weak dependence on the dimensionless cooling time, $\tau_{\rm cool}$, suggests that haloes meeting the heavy-seed criteria are typically subjected to an intense $J_{\rm LW}$ flux. For the majority of these haloes, $t_{\rm cool} \geq t_{\rm Hubble}$ throughout most of their early evolution, meaning that increasing $\tau_{\rm cool}$ from 0.05 to 1.0 has little influence on HSS frequency. Our mass ratio, $q = M_{\rm final}/M_{\rm initial}$, is used to keep the merger history of our candidates similar to Leo I, so that this criterion does not constrain dwarf galaxies hosting an HSS more generally. The results derived here for a given $\tau_{\rm cool}$ and $T_{\rm act}$ can therefore be thought of as a lower limit for HSS frequency in dwarf galaxies in general. For Leo-like haloes, we find that $q \sim 1.4$ optimizes the HSS frequency, where a large value results in very few or almost no mergers, and a smaller value can result in so many mergers that the Leo-like criteria are difficult to achieve.

The dominant parameter in this work is the threshold halo virial temperature $T_{\rm act}$ for atomic-cooling. Decreasing $T_{\rm act}$ below 9000 K dramatically increases the HSS frequency, implying that even small deviations from the canonical 10^4 K threshold can shift the outcome by orders of magnitude. Previous work has suggested that collapse could occur at lower virial temperatures, near $T_{\rm vir} \sim 8000$ K (J. A. Regan et al. 2020c). At this virial temperature, we derive an HSS frequency of $\sim$1 per cent (Fig. 3). Scenarios with $T_{\rm act} \leq 8000$ K are optimistic and not well-supported by current physical models; we retain them here to bracket the parameter space, but emphasize that such thresholds should be treated as speculative. Given the importance of this parameter, we here note several related points.

Our merger trees provide only the mass and redshift of haloes, and we assign a $T_{\rm vir}$ following equation (26) of R. Barkana & A. Loeb (2001). This value reflects the average depth of the corresponding gravitational potential in the spherical-collapse model, which would roughly correspond to the gas temperature in hydrostatic equilibrium. However, the true gas temperature in a cosmological halo with given mass $M_{\rm halo}$ at redshift z will vary from halo to halo, and is not necessarily equal to $T_{\rm vir}$ even on average. The relationship between the true gas temperature and the virial temperature, and the scatter of the gas temperature for similar atomic-cooling haloes, has not yet been fully characterized; some related discussion can be found in C. Shang et al. (2010). Further, the virial temperature represents an idealized scenario that does not consider effects that may cause rapid cooling and collapse to occur at lower temperatures. For example, in the `Renaissance` simulations, J. H. Wise et al. (2019) have identified two haloes in which H_2 cooling did occur and reduced the gas temperature below the atomic-cooling value. Nevertheless, these haloes experienced rapid mass inflows towards their core, above the critical

Downloaded from academic.oup.com/mnras/article/552/3/stag1839/8855713 by Institute of Science and Technology Austria user on 19 October 2026

value of $\sim 0.05 M_\odot yr^{-1}$ required for SMS formation (T. Hosokawa et al. 2013; L. Haemmerlé et al. 2018). In our work, non-negligible HSS frequencies require atomic cooling to set in near a virial-temperature threshold of $T_{act} \sim 7000$ K. Given the uncertainties discussed above, it is conceivable that a small fraction of haloes could reach this regime, though this remains speculative without direct numerical confirmation. This highlights the importance of follow-up work that investigates non-idealized gas dynamics for the onset of atomic cooling, considering effects such as turbulence, inflows, and anisotropies, as well as clarifying the scatter in T_{vir} for a given mass and redshift and the relationship between T_{vir} and gas temperature.

If Leo I indeed hosts a $M_\bullet \sim 10^6 M_\odot$ black hole as suggested by M. J. Bustamante-Rosell et al. (2021), its current BH-stellar mass ratio would be consistent with our evolved HSS predictions, $M_\bullet/M_* \sim 1$. We caution, however, that this ratio is not robustly established observationally, as discussed in Section 1. The long quenching time-scale (C. Gallart et al. 1999) and lack of mergers (F. Pacucci et al. 2023a) likely froze its mass ratio near the initial overmassive state, as we have found the ratio to slightly decrease but at a significantly slower rate than is typical for most DCBHs (M. T. Scoggins et al. 2022; M. T. Scoggins & Z. Haiman 2024).

We note that after completing the analysis for this work, another local dwarf galaxy, Segue 1, was recently modelled as having an extremely overmassive black hole (N. Lujan et al. 2025). The black hole is estimated to have mass $(4.5 \pm 1.5) \times 10^5 M_\odot$ and comparably very little stellar mass, $M_* \sim 10^3 M_\odot$ (M. Geha et al. 2009), resulting in a BH-to-stellar mass ratio of $M_\bullet/M_* \sim 10^2$. We note, however, that N. Lujan et al. (2025) employs a similar dynamical modelling methodology to M. J. Bustamante-Rosell et al. (2021), and the paper had not yet been accepted at the time of writing. Given the methodological concerns raised for Leo I by R. Pascale et al. (2024, 2025), this result should be treated with caution until independently confirmed with complementary data or methods. If confirmed, it would further support the idea that dwarf galaxies are excellent testing grounds for the $M_\bullet/M_*$ relations established in the early Universe.

We also highlight a previous work that also searches for massive black hole descendants in satellite galaxies. In S. Wassenhove et al. (2010), they investigate the occupation fraction for both massive and Pop III remnant black holes in MW satellites, not necessarily those that are similar to Leo I. They consider the effects of mass inflow on the formation of these massive seeds rather than explicitly modelling cooling and heating. They find that these massive black holes occupy less than a few per cent of the dwarf galaxies orbiting the MW, similar to the expected number of HSSs in Leo-like galaxies found in this work.

Finally, we briefly discuss the broader limitations of the model presented here. Beyond the T_{act} uncertainty discussed at length above, several other free parameters and assumptions warrant caution. The adopted virial mass for Leo I from M. Mateo et al. (2008) is uncertain, and as discussed in Section 2, more recent analyses suggest higher values; our HSS selection is directly sensitive to this choice. Given the steepness of the halo mass function near this range ($dN/dM \approx M^{-2}$), the $\sim$50 per cent higher masses favored by these more recent analyses would be expected to reduce the number of HSS candidates by a factor of a few. We also note that our black hole growth model assumes Eddington-limited accretion with fixed radiative efficiency and $f_{cap} = 0.05$. Because both the seed mass and the quenching cap scale linearly with f_{cap}, and most HSS black holes reach this cap well before $z = 0$ (Fig. 4), the predicted $M_\bullet/M_*$ ratio scales approximately linearly with f_{cap}, while the HSS occurrence frequency itself, set by the halo-selection criteria of Section 2.2, is unaffected by this choice. A different radiative efficiency would primarily shift the time-scale over which black holes approach this cap rather than its final value. Finally, the Leo-like selection criteria and in particular the number of required major mergers informed by T. Ruiz-Lara et al. (2021) introduce model dependence on the inferred star formation history of a single object.

5 CONCLUSIONS

Dwarf galaxies are thought to be ideal sites to probe potentially preserved $M_\bullet/M_*$ relations from high-z heavy-seed sites, with the local dwarf galaxy Leo I being one such exciting heavy-seed progenitor candidate. This work investigated this possibility by using Monte Carlo dark matter merger trees and the model developed in M. T. Scoggins & Z. Haiman (2024), to search for 'heavy-seed survivors', or DCBH sites that end up in a satellite halo similar to Leo I, orbiting a galaxy similar to the MW. We measure the HSS occurrence frequency as a function of the minimum allowed dimensionless cooling time, τ_{cool}, the halo virial temperature that defines the onset of rapid gas collapse in atomic-cooling haloes, T_{act}, and the minimum halo mass ratio for major mergers, q.

We find that, for virial temperature thresholds supported by the literature ($T_{act} \gtrsim 8000$ K), the formation of a heavy-seed descendant in Leo I is very unlikely, with an HSS frequency of $\sim$1 per cent. Only under highly optimistic and currently unsubstantiated assumptions on T_{act} does the probability become non-negligible. This possibility is also weakly dependent on q and τ_{cool}. Idealized conditions have set the canonical virial temperature for the onset of atomic cooling to $T_{act} = 10^4$ K, though recent work has found that this could be lower, closer to 8000 K (J. A. Regan et al. 2020c). Future work should aim to refine the details for the onset of rapid gas collapse in atomic cooling haloes, determining the scatter of the specific temperature at which atomic cooling begins, T_{act}, as well as the discrepancy between the estimated virial temperature and the gas temperature at the centre of the halo when it begins to collapse. In reality, the gas will not necessarily be in hydrostatic equilibrium in the halo's potential. Further, even if H_2 cooling does occur before reaching T_{act}, it is still possible to form an SMS, as long as the mass inflow exceeds the critical value of $\sim 0.05 M_\odot yr^{-1}$ required for SMS formation (T. Hosokawa et al. 2013; L. Haemmerlé et al. 2018; J. H. Wise et al. 2019). These effects mean our HSS frequency estimates at the canonical threshold should be treated as conservative, since the physical processes not included in our model could raise the true occurrence rate. However, we stress that this remains speculative without dedicated numerical follow-up, and we do not treat it as a demonstrated lower bound. The range of T_{act} explored below 8000 K should likewise be treated as speculative.

Overall, if Leo I does host a black hole of mass $\sim 10^6 M_\odot$ as suggested by M. J. Bustamante-Rosell et al. (2021), our results are consistent with a black hole-to-stellar mass ratio of $M_\bullet/M_* \sim 1$ for an evolved HSS. We stress, however, that the observational status of this black hole remains uncertain (see Section 1), and our results should be interpreted as characterizing the theoretical plausibility of this scenario rather than confirming it. Should the black hole be confirmed, Leo I and other similar dwarf galaxies that experienced few or no major mergers in their history would serve as local probes into high-redshift environments and potentially preserve the overmassive relation established at early times.

Downloaded from academic.oup.com/mnras/article/552/3/stag1839/8855713 by Institute of Science and Technology Austria user on 19 October 2026

ACKNOWLEDGEMENTS

We thank the anonymous reviewer for feedback that helped clarify this manuscript. ZH acknowledges support from NSF grant AST-2006176. FP acknowledges support from the Black Hole Initiative at Harvard University, which is funded by grants from the John Templeton Foundation and the Gordon and Betty Moore Foundation. Merger tree generation and analysis were performed with NSF's ACCESS allocations AST-120046 and AST-140041 on the Stampede3 resource. The freely available plotting library matplotlib (J. D. Hunter 2007) was used to construct the plots in this paper.

DATA AVAILABILITY

The code used to analyse the merger trees and generate figures for this manuscript is available at this GitHub repository. All other data will be shared upon reasonable request to the corresponding author.

REFERENCES

Abel T., Bryan G. L., Norman M. L., 2000, ApJ, 540, 39
Abel T., Bryan G. L., Norman M. L., 2002, Science, 295, 93
Agarwal B., Smith B., Glover S., Natarajan P., Khochfar S., 2016, MNRAS, 459, 4209
Bañados E. et al., 2018, Nature, 553, 473
Baggen J. F. W. et al., 2024, ApJ, 977, L13
Barkana R., Loeb A., 2001, Phys. Rep., 349, 125
Battaglia G., Sollima A., Nipoti C., 2015, MNRAS, 454, 2401
Boekholt T. C. N., Schleicher D. R. G., Fellhauer M., Klessen R. S., Reinoso B., Stutz A. M., Haemmerlé L., 2018, MNRAS, 476, 366
Bosman S. E. I., 2022, Zenodo
Bromm V., Loeb A., 2003, ApJ, 596, 34
Bromm V., Ferrara A., Coppi P., Larson R., 2001, MNRAS, 328, 969
Bustamante-Rosell M. J., Noyola E., Gebhardt K., Fabricius M. H., Mazzalay X., Thomas J., Zeimann G., 2021, ApJ, 921, 107
Cole S., Lacey C. G., Baugh C. M., Frenk C. S., 2000, MNRAS, 319, 168
Di Cintio P., Iorio G., Calura F., Nipoti C., Cantari M., 2024, A&A, 690, A61
Dijkstra M., Haiman Z., Mesinger A., Wyithe J. S. B., 2008, MNRAS, 391, 1961
Dijkstra M., Ferrara A., Mesinger A., 2014, MNRAS, 442, 2036
Escala A., 2021, ApJ, 908, 57
Fan X. et al., 2001, AJ, 122, 2833
Fan X. et al., 2003, AJ, 125, 1649
Fan X., Bañados E., Simcoe R. A., 2023, ARA&A, 61, 373
Gallart C., Freedman W. L., Aparicio A., Bertelli G., Chiosi C., 1999, AJ, 118, 2245
Geha M., Willman B., Simon J. D., Strigari L. E., Kirby E. N., Law D. R., Strader J., 2009, ApJ, 692, 1464
Glover S. C. O., 2015, MNRAS, 453, 2901
Greene J. E., 2012, Nature Commun., 3, 1304
Guia C. A., Pacucci F., Kocevski D. D., 2024, Res. Notes Am. Astron. Soc., 8, 207
Haemmerlé L., Woods T. E., Klessen R. S., Heger A., Whalen D. J., 2018, MNRAS, 474, 2757
Haiman Z., Rees M. J., Loeb A., 1997, ApJ, 476, 458
Harikane Y. et al., 2023, ApJ, 959, 39
Hayashi K., Chiba M., Ishiyama T., 2020, ApJ, 904, 45
Hirano S., Hosokawa T., Yoshida N., Umeda H., Omukai K., Chiaki G., Yorke H. W., 2014, ApJ, 781, 60
Hosokawa T., Yorke H. W., Inayoshi K., Omukai K., Yoshida N., 2013, ApJ, 778, 178
Hunter J. D., 2007, Comput. Sci. Eng., 9, 90
Inayoshi K., Haiman Z., Ostriker J. P., 2016, MNRAS, 459, 3738
Inayoshi K., Visbal E., Haiman Z., 2020, ARA&A, 58, 27
Inayoshi K., Onoue M., Sugahara Y., Inoue A. K., Ho L. C., 2022, ApJ, 931, L25
Iorio G., Nipoti C., Battaglia G., Sollima A., 2019, MNRAS, 487, 5692
Johnson J. L., Haardt F., 2016, Publ. Astron. Soc. Aust., 33, e007
Johnson J. L., Greif T. H., Bromm V., Klessen R. S., Ippolito J., 2009, MNRAS, 399, 37
Johnson J. L., Khochfar S., Greif T. H., Durier F., 2010, MNRAS, 410, 919
Katz O. Z., Redigolo D., Volansky T., 2025, J. Cosmol. Astropart. Phys., 2025, 047
Kocevski D. D. et al., 2023, ApJ, 954, L4
Kocevski D. D. et al., 2025, ApJ, 986, 126
Kokorev V. et al., 2024, ApJ, 968, 38
Kulkarni M., Visbal E., Bryan G. L., 2021, ApJ, 917, 40
Li J. et al., 2025, ApJ, 981, 19
Lodato G., Natarajan P., 2006, MNRAS, 371, 1813
Loeb A., Rasio F. A., 1994, ApJ, 432, 52
Lujan N. et al., 2025, ApJ, 992, L25
Lupi A., Haiman Z., Volonteri M., 2021, MNRAS, 503, 5046
Maiolino R. et al., 2024, A&A, 691, A145
Mateo M., Olszewski E. W., Walker M. G., 2008, ApJ, 675, 201
Matthee J. et al., 2024, ApJ, 963, 129
McConnachie A. W., 2012, AJ, 144, 4
Mezcua M., Siudek M., Suh H., Valiante R., Spinoso D., Bonoli S., 2023, ApJ, 943, L5
Mezcua M., Pacucci F., Suh H., Siudek M., Natarajan P., 2024, ApJ, 966, L30
Mortlock D. J. et al., 2011, Nature, 474, 616
Nakajima K., Maiolino R., 2022, MNRAS, 513, 5134
O'Shea B. W., Wise J. H., Xu H., Norman M. L., 2015, ApJ, 807, L12
Oh S. P., Haiman Z., 2002, ApJ, 569, 558
Oh S. P., Haiman Z., Rees M. J., 2001, ApJ, 553, 73
Pacucci F., Ferrara A., 2015, MNRAS, 448, 104
Pacucci F., Loeb A., 2019, ApJ, 870, L12
Pacucci F., Loeb A., 2022, ApJ, 940, L33
Pacucci F., Ni Y., Loeb A., 2023a, ApJ, 956, L37
Pacucci F., Nguyen B., Carniani S., Maiolino R., Fan X., 2023b, ApJ, 957, L3
Pacucci F., Hernquist L., Fujii M., 2025, ApJ, 994, 40
Parkinson H., Cole S., Helly J., 2007, MNRAS, 383, 557
Pascale R., Nipoti C., Calura F., Della Croce A., 2024, A&A, 684, L19
Pascale R., Nipoti C., Calura F., Della Croce A., 2025, A&A, 700, A77
Planck Collaboration, 2020, A&A, 641, A6
Press W. H., Schechter P., 1974, ApJ, 187, 425
Regan J., Volonteri M., 2024, Open J. Astrophys., 7, 72
Regan J. A., Haiman Z., Wise J. H., O'Shea B. W., Norman M. L., 2020a, Open J. Astrophys., 3, 1
Regan J. A., Wise J. H., Woods T. E., Downes T. P., O'Shea B. W., Norman M. C., 2020b, Open J. Astrophys., 3, 15
Regan J. A., Wise J. H., O'Shea B. W., Norman M. L., 2020c, MNRAS, 492, 3021
Regan J. A., Pacucci F., Bustamante-Rosell M. J., 2023, MNRAS, 518, 5997
Reines A. E., Volonteri M., 2015, ApJ, 813, 82
Ricarte A., Natarajan P., 2018, MNRAS, 481, 3278
Ruiz-Lara T. et al., 2021, MNRAS, 501, 3962
Ryu T., Tanaka T. L., Perna R., Haiman Z., 2016, MNRAS, 460, 4122
Schauer A. T. P., Glover S. C. O., Klessen R. S., Clark P., 2021, MNRAS, 507, 1775
Schleicher D. R. G. et al., 2022, MNRAS, 512, 6192
Scoggins M. T., Haiman Z., 2024, MNRAS, 531, 4584
Scoggins M. T., Haiman Z., Wise J. H., 2022, MNRAS, 519, 2155
Shang C., Bryan G. L., Haiman Z., 2010, MNRAS, 402, 1249
Tagawa H., Haiman Z., Kocsis B., 2020, ApJ, 892, 36
Tanaka T., Haiman Z., 2009, ApJ, 696, 1798
Tremmel M., Ricarte A., Natarajan P., Bellovary J., Sharma R., Quinn T. R., 2024, Open J. Astrophys., 7, 26

Downloaded from academic.oup.com/mnras/article/552/3/stag1839/8855713 by Institute of Science and Technology Austria user on 19 October 2026

Tumlinson J., Shull J. M., 2000, ApJ, 528, L65
van Wassenhove S., Volonteri M., Walker M. G., Gair J. R., 2010, MNRAS, 408, 1139
Vergara M. C., Escala A., Schleicher D. R. G., Reinoso B., 2023, MNRAS, 522, 4224
Volonteri M., 2010, A&AR, 18, 279
Volonteri M., Lodato G., Natarajan P., 2008, MNRAS, 383, 1079
Volonteri M., Habouzit M., Colpi M., 2021, Nat. Rev. Phys., 3, 732
Wang F. et al., 2021, ApJ, 908, 53
Weller E. J., Pacucci F., Natarajan P., Di Matteo T., 2023, MNRAS, 522, 4963
Wise J. H., Demchenko V. G., Halicek M. T., Norman M. L., Turk M. J., Abel T., Smith B. D., 2014, MNRAS, 442, 2560
Wise J. H., Regan J. A., O'Shea B. W., Norman M. L., Downes T. P., Xu H., 2019, Nature, 566, 85
Wolcott-Green J., Haiman Z., Bryan G. L., 2017, MNRAS, 469, 3329
Wu X.-B. et al., 2015, Nature, 518, 512
Xu H., Wise J. H., Norman M. L., Ahn K., O'Shea B. W., 2016, ApJ, 833, 84
Yang X. et al., 2020, ApJ, 904, 200

This paper has been typeset from a TEX/LATEX file prepared by the author.

Downloaded from academic.oup.com/mnras/article/552/3/stag1839/8855713 by Institute of Science and Technology Austria user on 19 October 2026

© The Author(s) 2026.
Published by Oxford University Press on behalf of Royal Astronomical Society. This is an Open Access article distributed under the terms of the Creative Commons Attribution License (https://creativecommons.org/licenses/by/4.0/), which permits unrestricted reuse, distribution, and reproduction in any medium, provided the original work is properly cited.